

Journal of Mechanics of Materials and Structures

**HOMOGENIZATION OF A VIERENDEEL GIRDER WITH ELASTIC JOINTS
INTO AN EQUIVALENT POLAR BEAM**

Antonio Gesualdo, Antonino Iannuzzo, Francesco Penta and Giovanni Pio Pucillo

Volume 12, No. 4

July 2017



HOMOGENIZATION OF A VIERENDEEL GIRDER WITH ELASTIC JOINTS INTO AN EQUIVALENT POLAR BEAM

ANTONIO GESUALDO, ANTONINO IANNUZZO, FRANCESCO PENTA AND GIOVANNI PIO PUCILLO

In this paper, a homogenization procedure of a Vierendeel girder with elastic joints is shown. The method is based on the Stephen transfer matrix analysis and employs (as a substitute continuum) a polar Timoshenko beam. The polar character of the equivalent beam arises quite naturally from the analysis of the pure bending eigenvector components of the girder force transfer matrix. Through the girder unit cell, two bending moments are transmitted: one is generated by the couple of axial forces acting on each nodal section of the beam, and the other is produced by the moments applied at the nodes of every section by the adjacent cells and is modeled as the resultant of the micropolar moments. Transfer force eigenvector analysis reveals that the unit cell bends while maintaining undeformed webs, a property that allows the evaluation of both the bending stiffnesses and the equivalent material micropolar scale parameter by means of straightforward equations.

The accuracy of the proposed method is verified by comparing the predictions of the homogenized model with literature data and with the results of the analysis of a series of girders carried out by the finite element method.

1. Introduction

Recently, in order to achieve simultaneously safety, sustainability and environmental compatibility, an increasing amount of attention has been paid to structural elements that are able to realize the optimal trade-off between strength and stiffness on one side, and lightness, economy and manufacturing times on the other.

A suitable example of a structural solution having these properties is the Vierendeel beam, which for this reason is often employed both in civil and industrial builds and in naval and aerospace constructions [Salmon et al. 2008; Tej and Tejová 2014; Nakayama 1985; Noor 1983; Cao et al. 2007]. The Vierendeel beam finds applications in railway structures as well. In fact, to design against the thermal track buckling phenomenon, rails, sleepers and fastenings are frequently modeled as a Vierendeel girder constrained to the ground by nonlinear springs, representative of the ballast actions [Kerr and Zarembski 1981; Pucillo 2016; De Iorio et al. 2014a; 2014b; 2014c].

The response of this kind of lattice beam to the service loads is usually analyzed in a CAE environment. The beam is reduced to a discrete system of finite elements and one of the solution methods for structural framework problems is then applied to it. If a great number of bays or unit cells composes the beam, it may be convenient to approximate its mechanical behavior by a continuum 1D model, whose properties are derived from those of the unit cell by a suitable homogenization method. In many cases, this kind

Keywords: Vierendeel girder, Timoshenko micropolar beam, transfer matrix analysis, homogenization, compliant joints, sensitivity analysis.

of approach offers the advantage of applying analytical solutions in closed form for the problem at hand. Moreover, the continuous approximation may be employed as a means of transition to a coarser discrete system with a smaller and more tractable set of kinematic and static unknowns.

However, the classical continuum theory does not provide an acceptable approximation and a micropolar theory has to be used in order to correctly analyze the in plane lattice bending. Several micropolar equivalent models have been reported in literature for the analysis of planar lattices [Noor 1988; Bazant and Christensen 1972; Kumar and McDowell 2004; Bakhvalov and Panasenko 1989; Hård af Segerstad et al. 2009; Wang and Stronge 1999; Warren and Byskov 2002; Onck 2002; Martinsson and Babuška 2007; Liu and Su 2009; Dos Reis and Ganghoffer 2012; Trovalusci et al. 2015; Bacigalupo and Gambarotta 2014; Hasanyan and Waas 2016]. However, studies on the micropolar models for analyzing beam-like lattices have not yet achieved the same advances. As far as the authors are aware, only two papers have specifically addressed this topic. In [Noor and Nemeth 1980], a rational approach was presented where stiffness parameters of the effective continuum model were obtained using energy equivalence concepts. Nodal displacements of the unit cell were obtained in an approximated way by a Taylor expansion of the kinematical model of the substitute continuum. Then, the equivalent stiffnesses were derived by equating the potential and kinetic energies of a unit cell of the lattice beam to those of the continuum. This approach leads to two questionable stiffness couplings: between the symmetric and antisymmetric components of the shear stresses and between the bending and couple stress moments. These make the solution of the equilibrium equations of the equivalent beam awkward for the simpler loading and constraining conditions. Furthermore, a key limitation of this research is that it does not take into account the girder joints elasticity.

More recently, Romanoff and Reddy [2014] used the modified couple stress Timoshenko beam theory [Ma et al. 2008; Reddy 2011] to analyze the transversal bending of web-core sandwich panels. The equivalent polar bending stiffness was determined by invoking the spring analogy criterion. According to this rule, along the substitute beam, the ratio of the couple stress moment to the total bending moment is given by the ratio of the chords' bending moments caused by the *thick face effect* to the moment of the couple of axial forces acting in the panels faces. As it will be shown, this assumption unfortunately leads to overestimates of the polar bending stiffness.

This article introduces an equivalent Timoshenko micropolar beam for the static analysis of Vierendeel girders with compliant joints. The adopted homogenization method is based on the force transfer matrix eigenanalysis presented in [Stephen and Wang 2000], where the homogenization of a truss made of hinged rods is also carried out as a numerical example. When this method is applied to the analysis of the girder, no approximations for the kinematical quantities nor subjective phenomenological assumptions on the inner moments are needed. The polar nature of the substitute beam is a direct consequence of the pure bending eigenvector structure of the force transfer matrix of the unit cell. Through the unit cell, two bending moments are transferred. The first one is generated by the axial forces acting on the nodal cross sections and corresponds to the Navier bending moment in the equivalent beam. The other one is due to the moments applied on the joints of the unit cell and is modeled by the polar moments. Furthermore, the ratio between the amplitudes of the two moments is such that the total moment is always transferred without deformations of the girder webs. On the basis of this property, equivalent bending stiffness and couple stress stiffness are expressed by means of a couple of surprisingly simple equations. These stiffnesses are also independent of the web properties, the cell length and the stiffness of web-chord

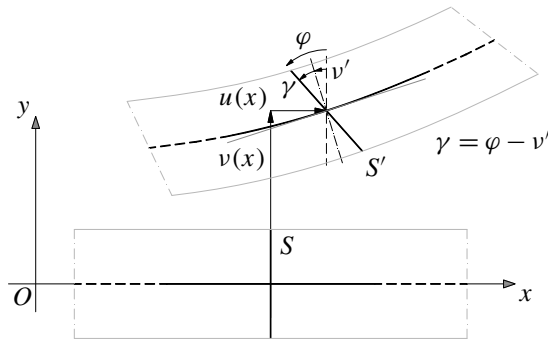


Figure 1. Kinematics of the Timoshenko beam.

joints, a result not yet reported in studies till now. Consequently, the polar material length scale ℓ is independent from the cell sizes and is a function only of the chords cross section geometry and material.

Finally, results from a validation study of the proposed model are also presented. The study has been carried out by means of both literature experimental data and the sensitivity analysis performed by finite element models.

2. The equivalent continuum

As an equivalent continuum, the modified polar Timoshenko beam is adopted [Ma et al. 2008; Reddy 2011]. The displacements (U, V) of a point $P(x, y)$ of the beam (see Figure 1) are given by

$$U = u(x) - y \cdot \varphi(x), \quad V = v(x),$$

where $u(x)$ and $v(x)$ denote respectively the longitudinal and transversal displacements of the beam axis and $\varphi(x)$ is the rotation of the cross section. The only nonzero strains at P are the normal strain in the x direction,

$$\varepsilon_x = \frac{du}{dx} - y \frac{d\varphi}{dx},$$

the shear strain associated with the directions x and y ,

$$\gamma_{xy} = \frac{dv}{dx} - \varphi(x),$$

and the curvature,

$$\chi_{xy} = \frac{1}{2} \frac{d\omega}{dx} = \frac{1}{4} \left(\frac{d\varphi}{dx} + \frac{d^2v}{dx^2} \right),$$

where $\omega = \frac{1}{2}(dv/dx + \varphi)$ is the rotation of an elementary neighborhood of P in the x - y plane.

Denoting by $\delta(\cdot)$ the kinematically admissible variations of the strain components and by σ_x , τ_{xy} and m_{xy} respectively the normal, tangential and the couple stress acting on the beam cross section, the virtual

strain energy or internal work can be expressed as

$$\begin{aligned} \delta U &= \int_l \int_A (\sigma_x \delta \varepsilon_x + \tau_{xy} \delta \gamma_{xy} + 2m_{xy} \delta \chi_{xy}) \, dA \, dx \\ &= \int_l \left[N_x \frac{d\delta u}{dx} + M_x \frac{d\delta \varphi}{dx} + Q_x \left(\delta \varphi - \frac{d\delta v}{dx} \right) + \frac{1}{2} P_{xy} \left(\frac{d\delta \varphi}{dx} + \frac{d^2 \delta v}{dx^2} \right) \right] dx, \end{aligned}$$

where l is the beam length and A is the area of its cross section,

$$N_x = \int_A \sigma_x \, dA, \quad Q_x = - \int_A \tau_{xy} \, dA, \tag{1}$$

are the beam axial and shear forces, while

$$M_x = - \int_A \sigma_x y \, dA \quad \text{and} \quad P_{xy} = \int_A m_{xy} \, dA \tag{2}$$

are the Navier and polar bending moments, respectively. It is worth nothing that the dual shear deformation of Q_x is

$$\gamma = -\gamma_{xy} = \varphi - \frac{dv}{dx}. \tag{3}$$

Under the assumption of homogeneous and isotropic linear elastic material, the stress-strain relationships are

$$\sigma_x = E \varepsilon_x, \quad \tau_{xy} = G \gamma_{xy}, \quad m_{xy} = 2G \ell^2 \chi_{xy},$$

with E being the Young modulus, G the tangential elasticity modulus and ℓ the material length scale parameter. Substituting the previous constitutive relations into the expressions of the stress resultants (1) and (2) gives

$$\begin{aligned} N_x &= A_{xx} \varepsilon_x, & Q_x &= D_Q \gamma, \\ M_x &= D_{xx} \frac{d\varphi}{dx}, & P_{xy} &= \frac{1}{2} S_{xy} \chi_{xy}, \end{aligned} \tag{4}$$

where A_{xx} and D_Q are respectively the axial and shear beam stiffnesses, $D_{xx} = EI$ is the bending stiffness, with I the second order central moment of the beam cross section, and $S_{xy} = 4G \ell^2 A$ the couple stress bending stiffness.

The beam equilibrium equations can be derived by equating the virtual internal work δU to the virtual work of the external loads, integrating by parts and taking into account the beam boundary conditions. For the simpler loading and constraint conditions, approximate solutions for these equations can be obtained by the Fourier series method (see [Reddy 2011] for more details).

3. Girder transfer matrix analysis and homogenization

In this section, the equivalent beam properties are evaluated by employing the transfer matrix analysis of a unit cell. So far, the transfer matrix methods have been applied mostly for the dynamic analysis of repetitive or periodic structures [Mead 1970; Meirovitch and Engels 1977; Yong and Lin 1989; Zhong and Williams 1995; Langley 1996]. Only recently have they also been used for the elasto-static analysis of prismatic, curved and pretwisted repetitive beam-like lattices made of pin-jointed bars [Stephen and Zhang 2004; 2006; Stephen and Ghosh 2005].

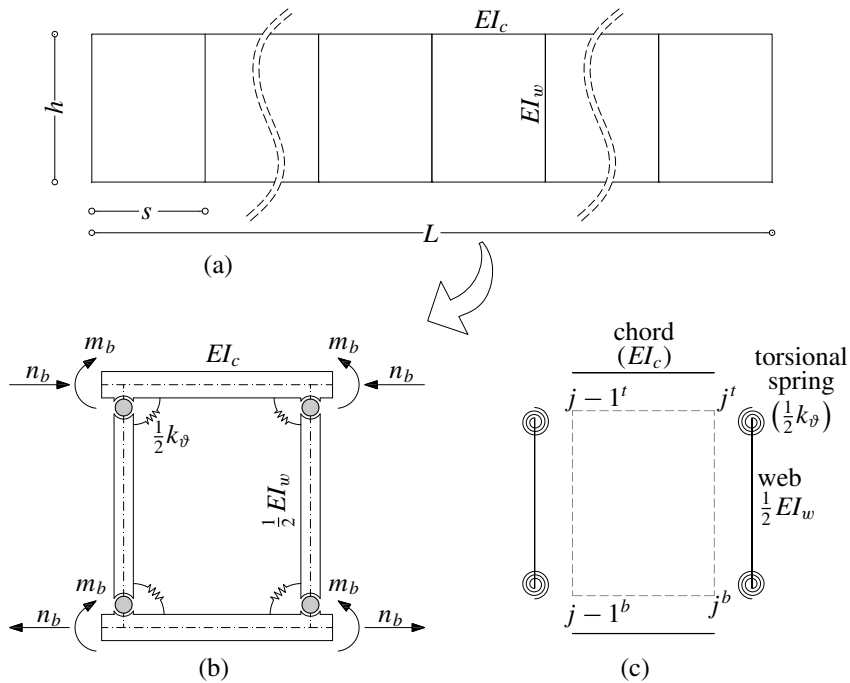


Figure 2. Vierendeel girder (a), unit cell (b) and exploded view of the elements composing the unit cell (c).

The main advantage of the method is that it allows evaluating both the Saint-Venant decay rates and the load transmission modes by carrying out an eigenanalysis of the transmission matrix G of the unit cell. Although it is conceptually simple, its practical implementation is problematic, since the G matrix is ill-conditioned and defective. Consequently, the Jordan block structure of G is very difficult to determine numerically. To overcome this problem, in this paper the force transfer matrix approach of Stephen and Wang [2000] is adopted. This method suppresses the redundant decay vectors and makes the assessment of the force transmission modes of the unit cell simpler.

In this study, the Vierendeel girder is modeled by assembling one-dimensional elements of Euler-Bernoulli type as represented in Figure 2. It consists of two straight parallel chords connected to the webs by means of torsional springs of stiffness k_ϑ . By these springs the elastic deformability of the web-chords' connections is taken into account. In Figure 2a the unit cell is depicted. Top and bottom chords have the same section, whose area and second order central moment are A_c and I_c , respectively. To respect the girder geometrical periodicity, cross sectional area and second order moment of the cell vertical beams are equal to the half part of the area A_w and second order moment I_w of the girder webs, while the stiffness of the unit cell torsional springs is $\frac{1}{2}k_\vartheta$.

In the following, we use the subscript j to identify any static or kinematic quantity concerning the nodal section j of the girder. Furthermore, to distinguish between the joints of a same section, we use superscripts t and b depending on whether the top or the bottom chords are involved. Coherently with this notation, the top and bottom joints of the section j are labeled $j^{(t)}$ and $j^{(b)}$.

For the sake of clarity, the nodal sections of the girder are numbered in such a way that sections $i - 1$

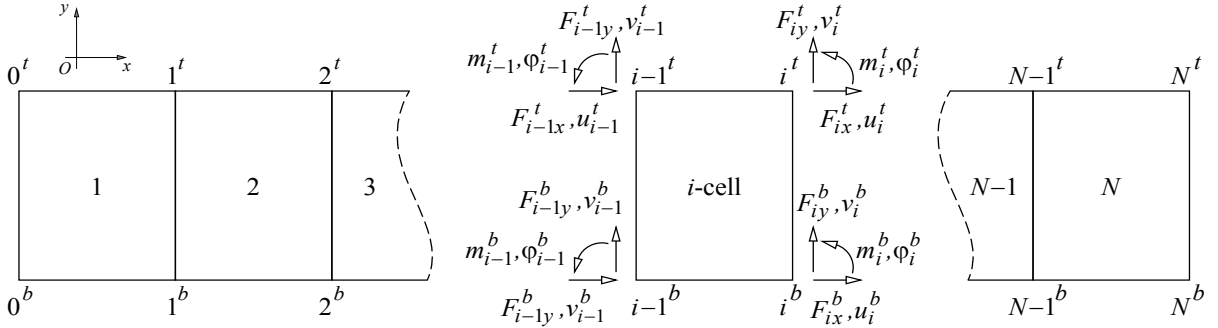


Figure 3. Unit cell nodes numbering with girder inner forces and nodal displacements.

and i bound the i -th cell respectively from the left and the right side, as shown in Figure 3. Therefore, the two extreme sections of a lattice beam of N cells are labeled correspondingly by 0 and N .

We denote with

$$s_j^t = [u_j^t, v_j^t, \varphi_j^t]^T \quad \text{and} \quad s_j^b = [u_j^b, v_j^b, \varphi_j^b]^T$$

the displacement vectors of the joints j^t and j^b , where $u_j^{(\cdot)}$ and $v_j^{(\cdot)}$ are the displacement components and $\varphi_j^{(\cdot)}$ the rotation of the joint $j^{(\cdot)}$. Therefore, the displacement vector of the nodal section j is $s_j = [s_j^{tT}, s_j^{bT}]^T$.

Similarly, the nodal forces applied on the joints j^t and j^b of the cell j are

$$p_j^t = [F_{jx}^t, F_{jy}^t, m_j^t]^T \quad \text{and} \quad p_j^b = [F_{jx}^b, F_{jy}^b, m_j^b]^T,$$

where $F_{jx}^{(\cdot)}$ and $F_{jy}^{(\cdot)}$ are respectively the axial and transversal components of the force and $m_j^{(\cdot)}$ the couple applied on the joint $j^{(\cdot)}$. Thus, the vector of the nodal forces acting on the section at the left side of the j -cell is

$$p_j = [p_j^{tT}, p_j^{bT}]^T.$$

In order to construct the displacement and force transfer matrix, we consider the couple of adjacent cells i and $i + 1$ sharing the nodal cross section i . By equilibrium, in absence of external loads on the section, the nodal forces on the left sides of the cell $i + 1$ are equal to $-p_i$.

The stiffness equations of the cells i and $i + 1$ in partitioned form are thus given by

$$\begin{bmatrix} -p_{i-1} \\ p_i \end{bmatrix} = \begin{bmatrix} K_{LL} & K_{LR} \\ K_{RL} & K_{RR} \end{bmatrix} \cdot \begin{bmatrix} s_{j-1} \\ s_j \end{bmatrix}, \tag{5}$$

$$\begin{bmatrix} -p_i \\ p_{i+1} \end{bmatrix} = \begin{bmatrix} K_{LL} & K_{LR} \\ K_{RL} & K_{RR} \end{bmatrix} \cdot \begin{bmatrix} s_j \\ s_{j+1} \end{bmatrix}, \tag{6}$$

in which subscripts L and R adopted for the subpartitions of the stiffness matrix refer to the left and right side of the cell. For the problem at hand, the cell stiffness matrix has been obtained following the standard method adopted in the finite element analyses, that is by assembling the stiffness matrix of the chords and those of the elastic systems composed by a cell vertical beam and the couple of torsional springs constraining it to the chords (see Figure 2c).

Adding the second equation in (5) to the first equation within (6) eliminates the vector \mathbf{p}_i , since we obtain

$$0 = \mathbf{K}_{RL} \mathbf{s}_{i-1} + (\mathbf{K}_{RR} + \mathbf{K}_{LL}) \mathbf{s}_i + \mathbf{K}_{LR} \mathbf{s}_{i+1}. \quad (7)$$

From the previous equation written for the section $(N - 1)$ of the girder, taking into account the boundary condition $s_N = 0$, the following relationship between the displacement vector \mathbf{s}_{N-1} and \mathbf{s}_{N-2} is deduced:

$$\mathbf{s}_{N-1} = -\mathbf{S}_1^{-1} \mathbf{K}_{RL} \mathbf{s}_{N-2},$$

where $\mathbf{S}_1 = \mathbf{K}_{RR} + \mathbf{K}_{LL}$.

Substituting this result within relation (7) specialized to the case of section $(N - 2)$, we have

$$\mathbf{s}_{N-2} = -\mathbf{S}_2^{-1} \mathbf{K}_{RL} \mathbf{s}_{N-3},$$

where $\mathbf{S}_2 = \mathbf{K}_{RR} + \mathbf{K}_{LL} - \mathbf{K}_{LR} \mathbf{S}_1^{-1} \mathbf{K}_{RL}$.

By iterating the previous algebraic operations until considering the section $j - 1$, the displacement vector \mathbf{s}_j of the inner section j can be expressed as function of the displacement vector \mathbf{s}_{j-1} of the adjacent nodal section by means of the equation

$$\mathbf{s}_j = \mathbf{S} \mathbf{s}_{j-1},$$

where \mathbf{S} is the j -cell displacement transfer matrix given by

$$\mathbf{S} = -\mathbf{S}_{N-j}^{-1} \mathbf{K}_{RL}, \quad (8)$$

with $\mathbf{S}_{N-j} = \mathbf{K}_{RR} + \mathbf{K}_{LL} - \mathbf{K}_{LR} \mathbf{S}_{(N-j+1)}^{-1} \mathbf{K}_{RL}$.

By expanding the stiffness matrix equation of the j -th cell and substituting in it the previous results, one obtains

$$\mathbf{p}_{j-1} = -\mathbf{K}_{LL} \mathbf{s}_{j-1} - \mathbf{K}_{LR} \mathbf{s}_j = -(\mathbf{K}_{LL} + \mathbf{K}_{LR} \mathbf{S}) \mathbf{s}_{j-1}, \quad (9a)$$

$$\mathbf{p}_j = \mathbf{K}_{RL} \mathbf{s}_{j-1} + \mathbf{K}_{RR} \mathbf{s}_j = (\mathbf{K}_{RL} + \mathbf{K}_{RR} \mathbf{S}) \mathbf{s}_{j-1}. \quad (9b)$$

Eliminating the displacement vector \mathbf{s}_{j-1} in (9) gives

$$\mathbf{p}_j = \mathbf{M} \mathbf{p}_{j-1},$$

where $\mathbf{M} = -(\mathbf{K}_{RL} + \mathbf{K}_{RR} \mathbf{S})(\mathbf{K}_{LL} + \mathbf{K}_{LR} \mathbf{S})^{-1}$ is the force transfer matrix of the cell j .

Notice that the matrix \mathbf{M} depends on the recurrence index j . It must have three unity eigenvalues corresponding to the force transmission modes and three nonunitary eigenvalues corresponding instead to the decay rates of self-equilibrated loadings [Stephen and Wang 2000]. However, when the j -index is not sufficiently high, numerical determination of the unitary eigenvector may be difficult or impossible. For the present analysis, a value of j equal to 100 has allowed the detection of the unit eigenvalues and the related eigenvectors with a precision of four decimal digits, at least.

Eigenspaces of \mathbf{M} associated to unit eigenvalues have dimensions 1 and 2. The one-dimensional eigenspace is related to the transmission of the beam axial force. Pure bending eigenvectors \mathbf{E}_b of the matrix \mathbf{M} belong instead to the eigenspace of dimension 2, since they may be coupled with the shear

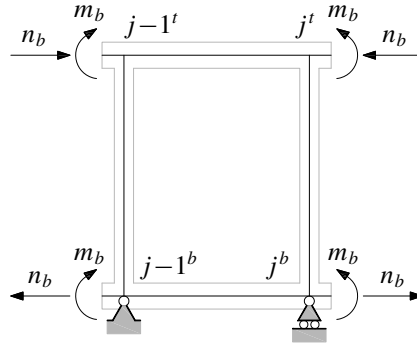


Figure 4. Unit cell under pure bending loading.

forces vector S_f . The latter is given by the chain rule defining the principal vector associated to the bending eigenvector E_b :

$$M \cdot E_b = E_b, \quad M \cdot S_f = E_b + S_f. \tag{10}$$

However, for the considered problem S_f can be obtained directly on the basis of very simple equilibrium considerations, without solving the algebraic problem defined by (10). In fact, it is worth noting that (9b) is the equilibrium relationship between the bending moments and the shear forces acting on a single cell.

The homogenized beam stiffnesses can be determined by averaging over the unit cell length s the cell responses under the load conditions defined by the unitary eigen- and principal vectors.

The eigenvector of the axial force E_a is

$$E_a = [n, 0, 0, n, 0, 0]^T.$$

Due to the symmetry of the cell, the two axial forces n are transmitted without bending; consequently only the chords deform with the axial elongations ns/EA_c . Thus, the equivalent axial stiffness of the homogenized beam is

$$A_{xx} = 2EA_c.$$

The pure bending eigenvector E_b has components

$$E_b = [-n_b, 0, m_b, +n_b, 0, m_b]^T,$$

where m and $\pm n_b$ are respectively the moments and the axial forces acting on the joints of the right side of the unit cell. The m moments correspond to the polar bending moment while the axial forces $\pm n_b$ generate the bending couple associated to the Navier moment in the Timoshenko polar beam.

To evaluate the equivalent bending stiffnesses, the cell displacements and rotations were calculated solving the elastic scheme of Figure 4. Denoting the upper and lower chords elongations respectively as $\Delta u_b = u_j^b - u_{j-1}^b$ and $\Delta u_t = u_j^t - u_{j-1}^t$, the mean curvature of the cell can be written in the form

$$\frac{1}{R} = \frac{\Delta u_b - \Delta u_t}{hs}.$$

Therefore, the equivalent bending stiffness D_{xx} is given by

$$D_{xx} = n_b h \cdot R = \frac{n_b h^2 s}{\Delta u_b - \Delta u_t}. \quad (11)$$

Polar bending stiffness can be evaluated by observing that when the shear force is zero, from (3) and (4) it follows that

$$\frac{d\varphi}{dX} = \frac{d^2 v}{dX^2}.$$

Hence, the polar and Navier moment of the homogenized beam make work by the same generalized strain, namely the beam curvature $d\varphi/dX$. For this reason, we evaluate the polar bending stiffness as

$$S_{xy} = 2m_b R = \frac{2m_b s h}{\Delta u_b - \Delta u_t}. \quad (12)$$

The principal vector of the shear forces is

$$S_f = [0, \frac{1}{2}T, 0, 0, \frac{1}{2}T, 0]^T,$$

where the shear resultant force T is obtained by the in plane rotation equilibrium of the unit cell

$$-Ts + n_b h + 2m_b = 0.$$

The equivalent shear stiffness is determined by analyzing the scheme in Figure 5. In it, the transversal load components of the principal vector S_f act on the left section of the unit cell, while on the right section, the axial forces vectors $\pm n_b$ and the moments m_b , given by the pure bending eigenvector E_b , are applied. Recalling the expression of the shear angle γ and denoting by

$$\hat{\varphi} = \frac{1}{4}(\varphi_{i-1}^{(t)} + \varphi_{i-1}^{(b)} + \varphi_i^{(t)} + \varphi_i^{(b)})$$

the average rotation angle of the cell and by

$$\frac{\Delta v}{s} = \frac{-v_{i-1}^{(t)} - v_{i-1}^{(b)}}{2s}$$

the mean slope of the cell center-line, the shear stiffness can be expressed as

$$D_Q = \frac{T}{\Delta v/s - \hat{\varphi}}. \quad (13)$$

Equations (11), (12) and (13) completely define the elastic behavior of the equivalent Timoshenko beam. The range of validity of these homogenized equations is analyzed in the next section on the basis of both literature experimental data and the numerical results of a sensitivity analysis.

4. Validation study

To verify the accuracy of the proposed micropolar beam, we use the experimental data from [Jutila and Romanoff 2007; Romanoff et al. 2007; 2009] as reported in [Romanoff and Reddy 2014]. They were obtained from specimens extracted from web-core sandwich panels. The specimens had unit cell length $s = 120$ mm, web height $h_w = 40$ mm, nominal web thickness $t_w = 4$ mm and were made of a steel

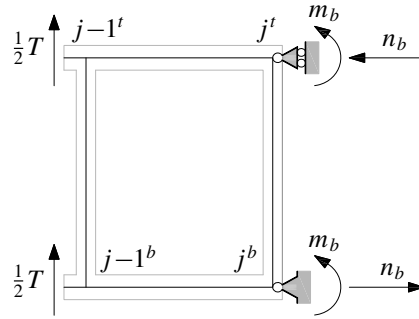


Figure 5. Unit cell under shear and bending loading.

having Young modulus $E = 200\text{--}220$ GPa and Poisson ratio $\nu = 0.3$. Top and bottom panels face plates had the same thickness $t = 2.5\text{--}3$ mm. A three point bending test was carried out on a beam of only 4 unit cells. Four point bending tests were executed on beams made of 9 and 15 unit cells. In these tests, the loads were applied at $\frac{1}{3}$ and at $\frac{2}{3}$ of the beam span L .

Only the deflection of the half-span section was measured for the 4 cell beam tested under the three points loading condition. For the 9 cell beam tested under the four points loading, the deflection was measured at the abscissas $X = 360$ mm. For the 15 cell beam having span $L = 1800$ mm, the deflections were instead measured at the abscissas $X = 200$ mm, $X = 400$ mm, $X = 600$ mm and $X = 1200$ mm. The measured deflections are listed in [Table 1](#), together with the stiffnesses and the deflections obtained under the assumption of plane strain by both the theory of Reddy–Romanoff and the model we propose. As it can be seen, the deflections predicted by the latter are in good agreement with the experimental data. It is worth noting that the bending and shear stiffnesses from the Reddy–Romanoff theory are very close to those of our model while the Reddy–Romanoff polar stiffness results are at least four times greater than the results obtained by the present method.

To study the accuracy of the predictions from the equivalent beam defined in [Section 3](#) in greater detail, it is essential to consider a wider data set than [[Romanoff and Reddy 2014](#)], including information on the effects of all the geometrical parameters influencing the girder response. To this end, a series of girder finite element models under the three points bending condition has been developed by assembling beam elements of Euler–Bernoulli type.

Given the properties of the chords and web cross-sections, as a first approximation the height h of the girder determines the relative importance of the two bending moments acting on its cross section. For this reason, in the first set of finite element analyses, the effects of different values of h for several values of the cell aspect ratio $\alpha = s/h$ and girder aspect ratio $\beta = L/h$ have been considered, under the assumption that the joints between chords and webs are rigid and that both chords and webs have the same cross section, specifically HEA100.

The results from these analysis are reported in [Figure 5](#) where the joints vertical displacements v_i of the girder finite element models having $h = 300, 600, 1200$ mm, $\alpha = 0.5, 1, 2$ and $\beta = 6, 12, 24, 48$ are compared with the elastic curves $v(x)$ of the corresponding homogenized beams. Previous values of h , α and β as well as the cross section properties were chosen in order to obtain a girder geometry similar to those encountered in the practice of structural design. The stiffnesses of the homogenized beams of [Figure 5](#) are listed in [Table 2](#) together with the corresponding values of the following nondimensional

	Unit	4 unit cells specimen [Jutila and Romanoff 2007]	9 unit cells specimen [Romanoff et al. 2009]	15 unit cell specimen [Romanoff et al. 2007]			
F	[N/m]	2000	4000	1000			
E	[GPa]	212	221	221			
ν		–	–	0.3			
B	[mm]	50	50	1000			
s	[mm]	120	120	120			
α	–	2.79	2.82	2.8			
β	–	4	9	15			
A_c	[mm ²]	152	126	2860			
I_c	[mm ³]	117	66.7	1950			
I_w	[mm ³]	273	261	5210			
k_J	[kN]	107	113	107			
D_{xx}	[kN m]	657 / 656	554 / 553	613 / 612			
D_Q	[kN/m]	388 / 500	304 / 368	355 / 447			
S_{xy}	[kN m]	4.33 / 1.09	2.57 / 0.648	3.61 / 0.908			
		$x/L = \frac{1}{2}$	$\frac{1}{3}$	$\frac{1}{9}$	$\frac{2}{9}$	$\frac{1}{3}$	$\frac{1}{2}$
$v(x/L)$	[mm]	0.487	4.69	0.675	1.33	1.9	2.02
		0.439	4.07	0.561	1.109	1.606	1.676
		0.446	4.14	0.750	1.37	1.88	2.02

Table 1. Top: geometrical details of 4, 9 and 15 unit cell specimens. Middle: values of D_{xx} , D_Q and S_{xy} obtained from the Reddy–Romanoff theory (before the slash) and with the present model (bold, after the slash). Bottom: Values of v for various x/L , obtained from the Reddy–Romanoff theory (first of three rows of results), the present theory (middle row, bold), and experiment (bottom row, slanted). Experimental and Reddy–Romanoff data are from [Romanoff and Reddy 2014].

measure of the homogenization error:

$$e = \left\{ \frac{1}{\bar{n}} \cdot \sum_{i \in \bar{N}} \left[\frac{v(x_i) - v_i}{v_i} \right]^2 \right\}^{1/2},$$

where \bar{N} is the set of \bar{n} nodes belonging to the inner model cross section of the girder and x_i is the abscissas of these nodes.

For all the girder aspect ratio considered, the homogenization error quickly decreases as the cell aspect ratio decreases or equivalently as the number of cell per beam unit length increases. This behavior is expected since the adopted method of homogenization is asymptotically exact; that is, $e \rightarrow 0$ when $\alpha/\beta = s/L \rightarrow 0$. The highest values of the homogenization error in Table 2 are attained when the girder aspect ratio β is equal to 6, namely when the girder is very stout and its behavior can be approximated only roughly by any beam model. Instead, the homogenization errors in Table 2 are much smaller for the more slender girders.

	α [-]	D_Q [Nmm ⁻¹]	S_{xy} [Nmm]	D_{xx} [Nmm]	e_{ave} [-]
$h = 300$ mm $\beta = 24$	0.50	$1.579 \cdot 10^8$	$1.481 \cdot 10^{12}$	$2.026 \cdot 10^{13}$	$8.233 \cdot 10^{-3}$
	1.00	$6.580 \cdot 10^7$	''	''	$5.312 \cdot 10^{-3}$
	2.00	$2.468 \cdot 10^7$	''	''	$1.107 \cdot 10^{-2}$
$h = 600$ mm $\beta = 12$	0.50	$3.948 \cdot 10^7$	$1.481 \cdot 10^{12}$	$8.105 \cdot 10^{13}$	$1.760 \cdot 10^{-2}$
	1.00	$1.645 \cdot 10^7$	''	''	$4.188 \cdot 10^{-2}$
	2.00	$6.169 \cdot 10^6$	''	''	$6.877 \cdot 10^{-2}$
$h = 1200$ mm $\beta = 6$	0.50	$9.871 \cdot 10^6$	$1.481 \cdot 10^{12}$	$3.242 \cdot 10^{14}$	$9.880 \cdot 10^{-2}$
	1.00	$4.113 \cdot 10^6$	''	''	$1.532 \cdot 10^{-1}$
	2.00	$1.542 \cdot 10^6$	''	''	$3.350 \cdot 10^{-1}$

Table 2. Equivalent stiffnesses and homogenization errors for Vierendeel girders with various heights H (span $L = 7600$ mm, chords and web sections: HEA100).

	webs [-]	D_Q [Nmm ⁻¹]	S_{xy} [Nmm]	D_{xx} [Nmm]	e_{ave} [-]
$h = 300$ mm $\alpha = 0.5$ $\beta = 24$	HEA100	$3.131 \cdot 10^7$	$2.570 \cdot 10^{12}$	$2.417 \cdot 10^{13}$	$8.465 \cdot 10^{-3}$
	HEA120	$4.284 \cdot 10^7$	''	''	$1.739 \cdot 10^{-3}$
	HEA140	$5.399 \cdot 10^7$	''	''	$1.553 \cdot 10^{-3}$
	HEA160	$6.289 \cdot 10^7$	''	''	$2.283 \cdot 10^{-3}$
$h = 600$ mm $\alpha = 1.0$ $\beta = 12$	HEA100	$1.955 \cdot 10^7$	$2.570 \cdot 10^{12}$	$9.670 \cdot 10^{13}$	$4.456 \cdot 10^{-2}$
	HEA120	$2.906 \cdot 10^7$	''	''	$3.145 \cdot 10^{-2}$
	HEA140	$3.997 \cdot 10^7$	''	''	$1.810 \cdot 10^{-2}$
	HEA160	$5.719 \cdot 10^7$	''	''	$2.623 \cdot 10^{-2}$

Table 3. Equivalent stiffnesses and homogenization errors for Vierendeel girders with webs of various cross section (span $L = 7600$ mm, chords' sections: HEA120).

In [Figure 6](#) and in [Table 3](#) the effects of the variations of the web bending stiffness on the accuracy of the proposed beam model are analyzed for two values of the girder aspect ratio β . It is evident that the homogenization error follows the same trend for both values of β , attaining the greater values when the webs have the lower shear stiffness. However, in both cases, the errors are negligible and are acceptable for engineering purposes, being less than or equal to 5%.

In [Figure 6](#) the elastic lines of the homogenized beam models by Noor–Nemeth [1980] and Romanoff–Reddy [2014] are also reported for comparison purposes. As it can be seen, the Reddy–Romanoff theory in all the examined cases underestimates the finite element model's displacements while the predictions of the proposed approach are affected by an error of the same order of magnitude as the error of the Noor–Nemeth theory.

Also when the joints between webs and chords are elastically compliant, the predictions from our beam model are in excellent agreement with the finite element method results for a wide range of values of the joint compliance. This is evident from results reported in [Figure 7](#), where the vertical displacements of a series of girder finite element models having various stiffnesses of the torsional springs are compared

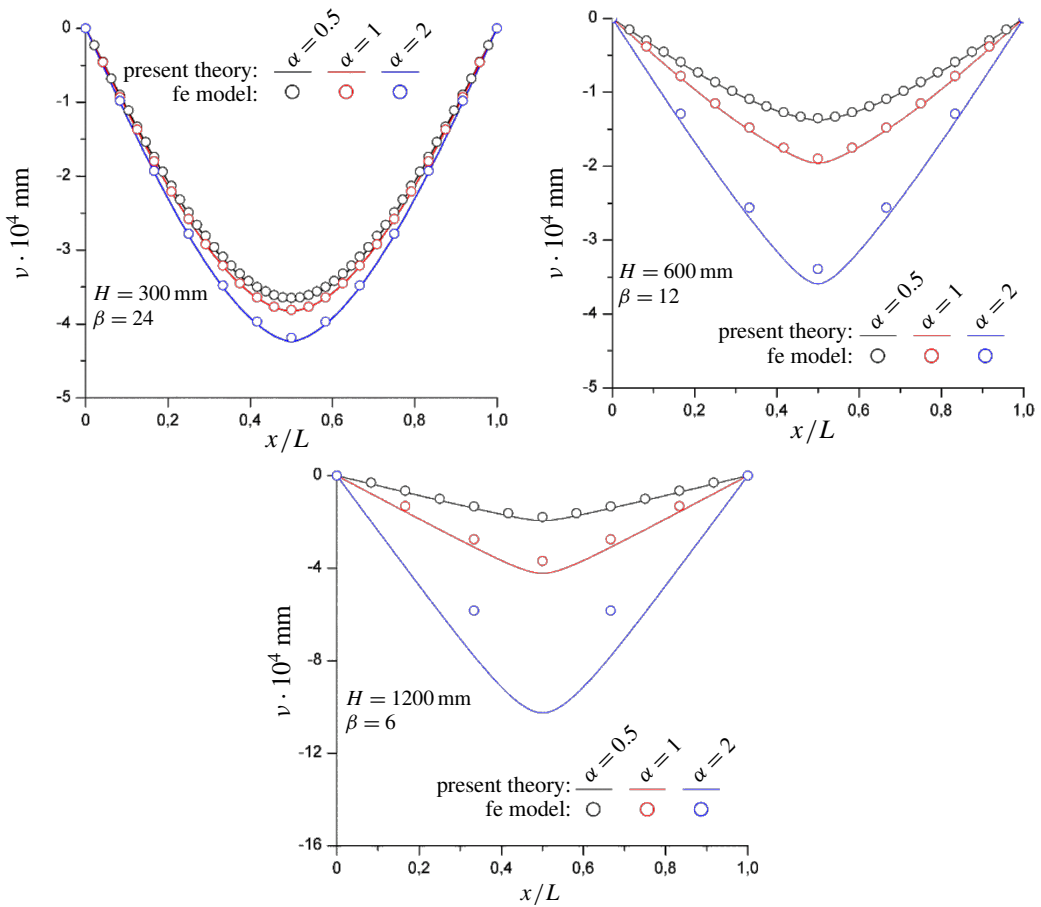


Figure 6. Vertical deflections of Vierendeel girders finite element models and elastic lines of the equivalent Timoshenko beams: effects of girder height H (span $L = 7600$ mm, chords and web sections HEA100).

with the elastic lines of the corresponding homogenized polar beam. The spring stiffness values of these girders have been chosen in order to realize, starting from the ideal case of perfectly rigid chord-webs joints, percent increments χ equal to 1, 5, 25, 50, 100, 400 and 2000 for the bending compliance of the elastic systems of Figure 2c. As schematically shown in Figure 7, the systems are composed by a web in series with the corresponding springs constraining it to the chords. In Table 4, the stiffnesses and the homogenization errors of the equivalent beam of Figure 7 are listed.

The influence that both web shear and joint stiffnesses have on the homogenization error can be explained as follows: recall that in a Vierendeel girder the bending constraint action that the chords exert on each other depends on these stiffnesses, being the Vierendeel effect directly proportional to them. In other words, for lower values of the web shear and joint stiffnesses, the jumps in the chords' axial forces at the girder joints become smaller; as a result, when either EI_w or k_θ decrease, the girder behavior tends toward an Euler–Bernoulli beam, having infinite shear stiffness and bending stiffness equal to the one

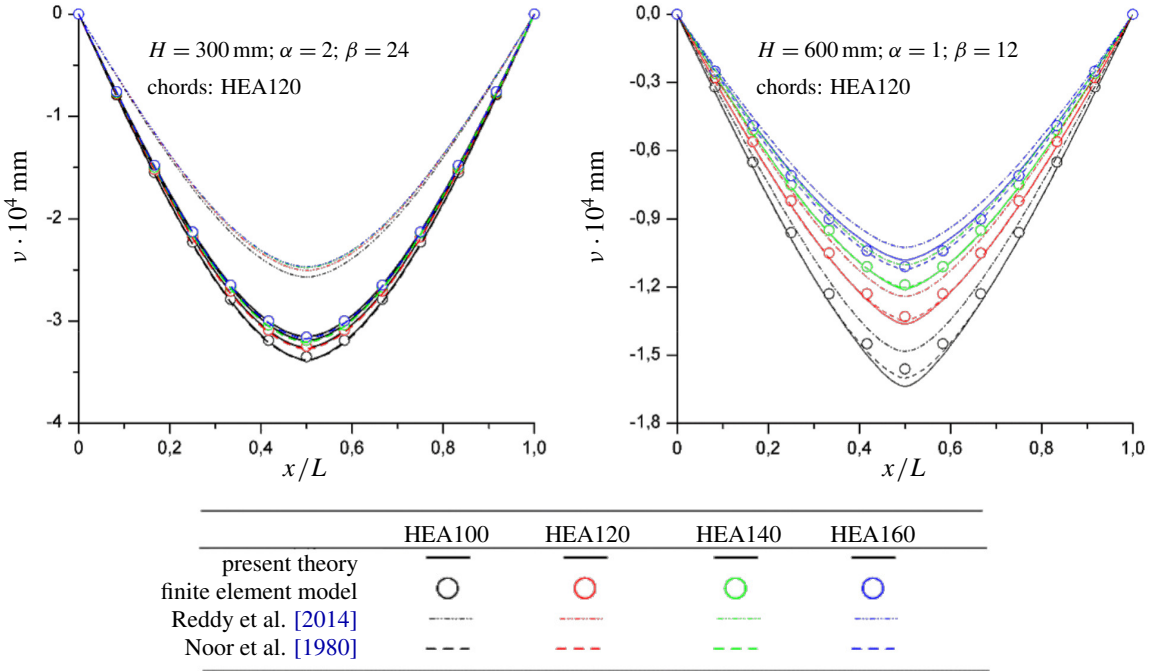


Figure 7. Vertical deflections of Vierendeel girders finite element models and elastic lines of the equivalent Timoshenko beams: effects of the girder webs cross sections.

	χ % [-]	k_{ϑ} [Nmm]	D_Q [Nmm ⁻¹]	S_{xy} [Nmm]	D_{xx} [Nmm]	e_{ave} [-]
$h = 300$ mm $\alpha = 2.0$ $\beta = 24$ chords = HEA100 webs = HEA100	1.0	$7.403 \cdot 10^{11}$	$2.530 \cdot 10^7$	$1.481 \cdot 10^{12}$	$2.026 \cdot 10^{13}$	$4.681 \cdot 10^{-3}$
	5.0	$1.481 \cdot 10^{11}$	$2.437 \cdot 10^7$	"	"	$5.925 \cdot 10^{-3}$
	25.0	$2.961 \cdot 10^{10}$	$2.058 \cdot 10^7$	"	"	$1.067 \cdot 10^{-2}$
	50.0	$1.481 \cdot 10^{10}$	$1.724 \cdot 10^7$	"	"	$1.360 \cdot 10^{-2}$
	100.0	$7.403 \cdot 10^9$	$1.300 \cdot 10^7$	"	"	$1.558 \cdot 10^{-2}$
	400.0	$1.851 \cdot 10^9$	$5.258 \cdot 10^6$	"	"	$5.639 \cdot 10^{-2}$
	2000.0	$3.702 \cdot 10^8$	$1.259 \cdot 10^6$	"	"	$1.881 \cdot 10^{-1}$
$h = 1200$ mm $\alpha = 0.5$ $\beta = 12$ chords = HEA160 webs = HEA160	1.0	$8.867 \cdot 10^{11}$	$4.655 \cdot 10^7$	$7.094 \cdot 10^{12}$	$5.918 \cdot 10^{14}$	$2.266 \cdot 10^{-2}$
	5.0	$1.773 \cdot 10^{11}$	$4.379 \cdot 10^7$	"	"	$2.317 \cdot 10^{-2}$
	25.0	$3.547 \cdot 10^{10}$	$3.378 \cdot 10^7$	"	"	$3.196 \cdot 10^{-2}$
	50.0	$1.773 \cdot 10^{10}$	$2.627 \cdot 10^7$	"	"	$4.158 \cdot 10^{-2}$
	100.0	$8.867 \cdot 10^9$	$1.819 \cdot 10^7$	"	"	$5.035 \cdot 10^{-2}$
	400.0	$2.217 \cdot 10^9$	$6.392 \cdot 10^6$	"	"	$9.207 \cdot 10^{-2}$
	2000.0	$4.433 \cdot 10^8$	$1.433 \cdot 10^6$	"	"	$2.144 \cdot 10^{-1}$

Table 4. Equivalent stiffnesses and homogenization errors for Vierendeel girders with elastic joints: effects of the joints stiffness (span $L = 7600$ mm).

of the two chords acting in parallel. However, when EI_w or k_ϑ become very small, the shear stiffness of the unit cell tends to the minimum value $3EI_c/s^3$ and consequently the Timoshenko beam model over-estimates the real displacements.

5. Analysis of results

Results listed in Tables 2, 3 and 4 clearly show that the bending and polar stiffnesses evaluated by the present method appear to be independent from the web bending stiffness and the stiffness k_ϑ of the torsional springs. For fixed values of the girder aspect ratio β , D_{xx} and S_{xy} are insensitive to any changes of the cell aspect ratio α . Moreover, given the girder span L , these stiffnesses do not change for changes in the ratio $\alpha/\beta = s/L$. This is in marked contrast to results of previous theories for homogenizing toward a polar beam, whose equivalent stiffnesses have the expressions reported in Table 5.

Indeed, the aforementioned property of D_{xx} and S_{xy} are a consequence of the deformation mode by which the cell transfers the bending moment to the neighboring cells. Actually, the cell bends while maintaining its webs in the straight configuration, a fact that allows the determination of the equivalent bending stiffnesses without executing the eigenanalysis of the transfer matrix \mathbf{M} .

For this aim, we first observe that the unit cell is symmetric with respect to the vertical and horizontal centroidal axes; see Figure 2b. Under the loading condition defined by the pure bending eigenvector (see Figure 4), the bending moments at the ends of the chords and webs have the same amplitudes, respectively m_c and m_w . Hence, the corresponding cell equilibrium configuration (Figure 9) is defined by equilibrium equations of the joints having the form

$$m_b = m_c - m_w \tag{14}$$

and by the inner compatibility conditions

$$\varphi_{j(w)}^q = \varphi_{j(c)}^q, \text{ with } q = t, b, \tag{15}$$

where $\varphi_{j(w)}^q$ and $\varphi_{j(c)}^q$ are respectively the rotations of the web and chord end sections at the joint j^q . These rotations have expressions given by

$$\varphi_{j(c)}^{(q)} = \pm \frac{m_c s}{2EI_c}, \quad \varphi_{j(w)}^{(q)} = \pm \left(\psi - \frac{m_w s}{6EI_w} \right), \tag{16}$$

where the angles

$$\psi = \pm \frac{\Delta u_b - \Delta u_t}{2h} = \pm \frac{n_b s}{EA_c h} \tag{17}$$

	D_{xx}	S_{xy}
Reddy–Romanoff theory [Romanoff and Reddy 2014]	$\frac{1}{2}EA_c h^2 + 2EI_c$,	$\frac{8(I_c D_{xx})}{(\frac{1}{2}EA_c h^2 + \delta EI_w)}$, $\delta = \left(\frac{I_w}{2I_c} + 12 \frac{EI_w}{k_\vartheta s} + \frac{h}{s} \right)^{-1}$
Noor–Nemeth theory [Noor and Nemeth 1980]	$\frac{1}{2}EA_c h^2 + 3EI_w \frac{s}{h}$	$2EI_c + 3EI_w \frac{s}{h}$

Table 5. Equivalent bending and polar stiffnesses of a Vierendeel girder.

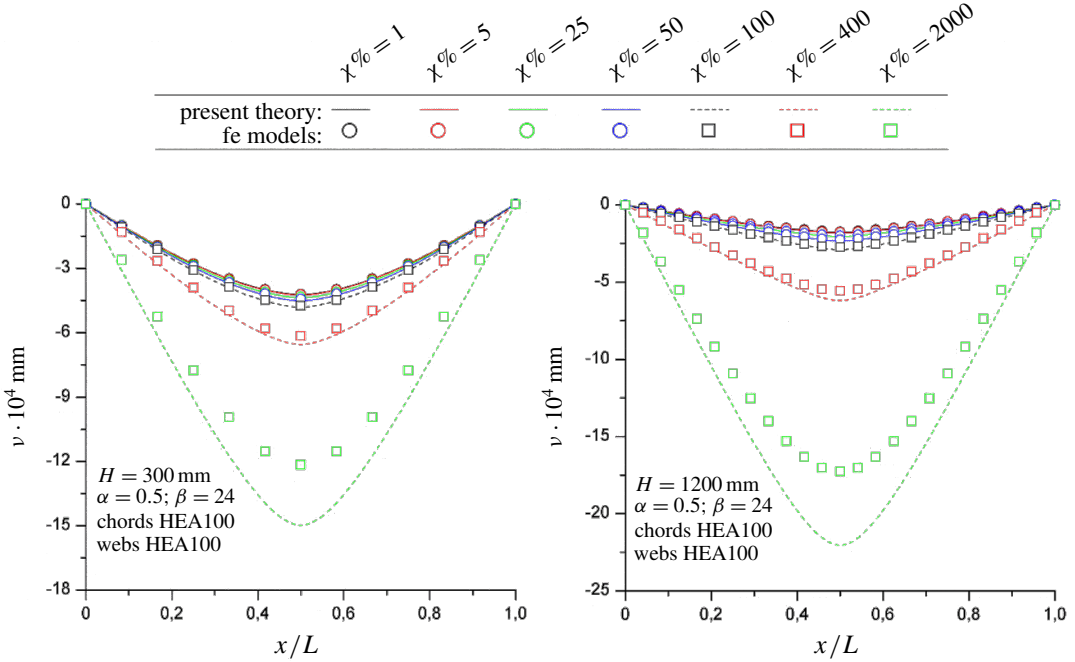


Figure 8. Vertical deflections of Vierendeel girders fe models and elastic lines of the equivalent Timoshenko beams: effects of joint elasticity.

are the web’s rigid rotations that would occur as a consequence of the chords elongations if the webs were simply hinged to the chords. According to the sign convention of Figure 9, the choice of +/− in the previous equations depends on whether joints on the right or on the left side of the cell are considered. Through (14)–(16), it can be recognized that the cell equilibrium can be attained without deformations of the webs, that is with $m_w = 0$, only if

$$\varphi_{j(w)}^q = \varphi_{j(c)}^q = \psi \quad \text{and} \quad m_b = m_c = \frac{2n_b I_c}{A_c h}. \tag{18}$$

When previous conditions are met, the curvature of the chords is given by

$$\frac{1}{R} = \frac{2\psi}{s} = \frac{2n_b}{EA_c h}.$$

Substituting this result into (11) and (12) and taking into account (18), we obtain the following expressions of the bending and polar stiffnesses of the equivalent beam:

$$\begin{aligned} D_{xx} &= \frac{n_b h s}{2\psi} = \frac{1}{2} EA_c h^2, \\ S_{xy} &= \frac{2m_b s}{2\psi} = 2EI_c. \end{aligned} \tag{19}$$

The stiffnesses evaluated by previous formulas perfectly match those listed in Tables 1–4, which were obtained by the numerical procedure in Section 4.

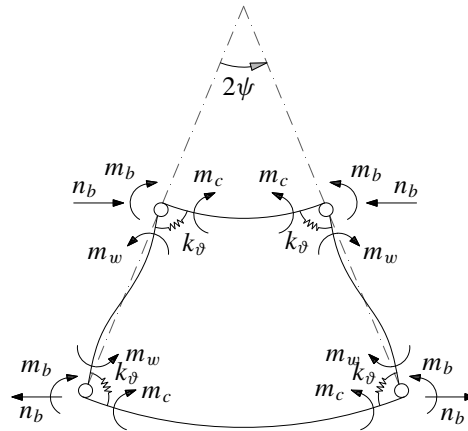


Figure 9. Unit cell deformed shape under pure bending loads.

Finally, equating the expression of S_{xy} given in (19) to the polar stiffness of a Timoshenko beam, the following expression for the material length scale ℓ is derived:

$$\ell = \rho_c \sqrt{1 + \nu},$$

where ρ_c is the central (inertial) radius of gyration of the chord cross section. According to this latter result, the severity of the polar effect in the equivalent Timoshenko beam appears to be totally independent from the cell sizes and is a function only of the chords cross section geometry and the girder material.

6. Conclusions

The homogenization of a Vierendeel girder having elastic joints has been performed by adopting a Timoshenko polar beam as substitute medium. The equivalent stiffnesses were determined by a numerical procedure based on the analysis of the eigen- and principal vectors of the force transfer matrix of the unit cell. While previous approaches proposed that the polar character of the beam is deduced by kinematical conjectures or is inspired by the microstructure, in the present study it is a direct consequence of the pattern of the inner forces acting in the lattice when the pure bending mode of the cell is active.

The method we proposed has been validated on the basis of some experimental data from literature and the results of a series of finite element models. In almost all the examined cases, the predictions of our model were in good agreement with numerical and experimental outcomes. Furthermore, from the validation study, we found that the bending and polar stiffnesses are independent from the web bending stiffness and do not change with either the unit cell length s or the stiffness k_θ of the torsional springs. In addition, the bending moment is transferred by the unit cell without deformation of the webs; during bending, the webs maintain their initial straight configuration. From this result, two simple formulas for the bending and polar stiffness were derived.

The presented beam model has great potential for analyzing the behavior of any beam-like repetitive structures with elastic or rigid joints. More specifically, it appears to be a serious candidate for analyzing the buckling and postbuckling response of infinitely long periodic beams, such as the railway track under thermal load. Its range of validity is bounded by the bending stiffness of the webs and the stiffness

of the web-chord connections. As these stiffnesses decrease, from the presented theory a family of Timoshenko beams having increasing shear flexibility are obtained. However, in real girders, the smaller these stiffnesses are, the weaker the Vierendeel effect results. As a consequence, the girder behavior tends toward an Euler–Bernoulli beam having bending stiffness equal to twice the chord bending stiffness. However, the extension of the proposed approach to girders with weak Vierendeel effects needs a deeper analysis and probably will be the object of future research.

Similarly, further research will be needed to apply the proposed model in the girder elasto-plastic range, where the response of the unit cell has to be analyzed by approximated methods, as presented in [Fraldi et al. 2010; 2014].

References

- [Bacigalupo and Gambarotta 2014] A. Bacigalupo and L. Gambarotta, “Homogenization of periodic hexa- and tetrachiral cellular solids”, *Compos. Struct.* **116** (2014), 461–476.
- [Bakhvalov and Panasenko 1989] N. Bakhvalov and G. Panasenko, *Averaging processes in periodic media: mathematical problems in the mechanics of composite materials*, Mathematics and its Applications **36**, Kluwer Academic Publishers, Dordrecht, The Netherlands, 1989.
- [Bazant and Christensen 1972] Z. Bazant and M. Christensen, “Analogy between micropolar continuum and grid frameworks under initial stress”, *Int. J. Solids Struct.* **8** (1972), 327–346.
- [Cao et al. 2007] J. Cao, J. L. Grenestedt, and W. J. Maroun, “Steel truss/composite skin hybrid ship hull, I: design and analysis”, *Compos. A Appl. Sci. Manuf.* **38** (2007), 1755–1762.
- [De Iorio et al. 2014a] A. De Iorio, M. Grasso, F. Penta, G. P. Pucillo, P. Pinto, S. Rossi, M. Testa, and G. Farneti, “Transverse strength of railway tracks, I: planning and experimental setup”, *Frattura ed Integrità Strutturale* **30** (2014), 478–485.
- [De Iorio et al. 2014b] A. De Iorio, M. Grasso, F. Penta, G. P. Pucillo, and V. Rosiello, “Transverse strength of railway tracks, II: test system for ballast resistance in line measurement”, *Frattura ed Integrità Strutturale* **30** (2014), 578–592.
- [De Iorio et al. 2014c] A. De Iorio, M. Grasso, F. Penta, G. P. Pucillo, V. Rosiello, S. Lisi, S. Rossi, and M. Testa, “Transverse strength of railway tracks, III: multiple scenarios test field”, *Frattura ed Integrità Strutturale* **30** (2014c), 593–601.
- [Dos Reis and Ganghoffer 2012] F. Dos Reis and J. F. Ganghoffer, “Construction of micropolar continua from the asymptotic homogenization of beam lattices”, *Comput. Struct.* **112** (2012), 354–363.
- [Fraldi et al. 2010] M. Fraldi, L. Nunziante, A. Gesualdo, and F. Guarracino, “On the bounding of limit multipliers for combined loading”, *Proc. R. Soc. Lond. A* **466**:2114 (2010), 493–514.
- [Fraldi et al. 2014] M. Fraldi, A. Gesualdo, and F. Guarracino, “Influence of actual plastic hinge placement on the behavior of ductile frames”, *J. Zhejiang Univ. Sci. A* **15** (2014), 482–495.
- [Hasanyan and Waas 2016] A. Hasanyan and A. Waas, “Micropolar constitutive relations for cellular solids”, *J. Appl. Mech. (ASME)* **83** (2016), art. id. 041001, pp. 10.
- [Jutila and Romanoff 2007] M. Jutila and J. Romanoff, *Laserhitsatun teräksisen kerroslevypalkin kolmipistetaivutus-kokeet*, master’s thesis, Helsinki University of Technology, 2007.
- [Kerr and Zarembski 1981] A. D. Kerr and A. M. Zarembski, “The response equations for a cross-tie track”, *Acta Mech.* **40** (1981), 253–276.
- [Kumar and McDowell 2004] R. S. Kumar and D. L. McDowell, “Generalized continuum modeling of 2-D periodic cellular solids”, *Int. J. Solids Struct.* **41** (2004), 7399–7422.
- [Langley 1996] R. S. Langley, “A transfer matrix analysis of the energetics of structural wave motion and harmonic vibration”, *Proc. R. Soc. Lond. A* **452** (1996), 1631–1648.
- [Liu and Su 2009] S. Liu and W. Su, “Effective couple-stress continuum model of cellular solids and size effects analysis”, *Int. J. Solids Struct.* **46** (2009), 2787–2799.

- [Ma et al. 2008] H. M. Ma, X.-L. Gao, and J. N. Reddy, “A microstructure-dependent Timoshenko beam model based on a modified couple stress theory”, *J. Mech. Phys. Solids* **56**:12 (2008), 3379–3391.
- [Martinsson and Babuška 2007] P.-G. Martinsson and I. Babuška, “Mechanics of materials with periodic truss or frame microstructures”, *Arch. Ration. Mech. Anal.* **185**:2 (2007), 201–234.
- [Mead 1970] D. J. Mead, “Free wave propagation in periodically-supported infinite beams”, *J. Sound Vib.* **13** (1970), 181–197.
- [Meirovitch and Engels 1977] L. Meirovitch and R. C. Engels, “Response of periodic structures by the Z-transform method”, *AIAA J.* **15**:2 (1977), 167–174.
- [Nakayama 1985] Y. Nakayama, “Aerodynamic stability of cable-stayed bridge with new Vierendeel-type girder”, *Eng. Struct.* **7** (1985), 85–92.
- [Noor 1983] A. K. Noor, “Assessment of current state of the art in modeling techniques and analysis methods for large space structures”, pp. 5–32 in *NASA Conference Publication 2258* (Williamsburg, VA, 1982), edited by L. D. Pinson et al., 1983.
- [Noor 1988] A. K. Noor, “Continuum modeling for repetitive lattice structures”, *Appl. Mech. Rev. (ASME)* **41** (1988), 285–296.
- [Noor and Nemeth 1980] A. K. Noor and M. P. Nemeth, “Micropolar beam models for lattice grids with rigid joints”, *Comput. Methods Appl. Mech. Eng.* **21** (1980), 249–263.
- [Onck 2002] P. R. Onck, “Cosserat modeling of cellular solids”, *C. R. Mécanique* **330** (2002), 717–722.
- [Pucillo 2016] G. P. Pucillo, “Thermal buckling and post-buckling behaviour of continuous welded rail track”, *Veh. Syst. Dyn.* **54** (2016), 1785–1807.
- [Reddy 2011] J. N. Reddy, “Microstructure-dependent couple stress theories of functionally graded beams”, *J. Mech. Phys. Solids* **59**:11 (2011), 2382–2399.
- [Romanoff and Reddy 2014] J. Romanoff and J. N. Reddy, “Experimental validation of the modified couple stress Timoshenko beam theory for web-core sandwich panels”, *Compos. Struct.* **111** (2014), 130–137.
- [Romanoff et al. 2007] J. Romanoff, H. Remes, G. Socha, M. Jutila, and P. Varsta, “The stiffness of laser stake welded T-joints in web-core sandwich structures”, *Thin-Walled Struct.* **45** (2007), 453–462.
- [Romanoff et al. 2009] J. Romanoff, A. Laakso, and P. Varsta, *Improving the shear properties of web-core sandwich structures using filling material: analysis and design of marine structures*, CRC Press, Leiden, The Netherlands, 2009.
- [Salmon et al. 2008] G. C. Salmon, J. E. Johnson, and F. A. Malhas, *Steel structures: design and behavior*, 5th ed., Prentice Hall, 2008.
- [Hård af Segerstad et al. 2009] P. Hård af Segerstad, S. Toll, and R. Larsson, “A micropolar theory for the finite elasticity of open-cell cellular solids”, *Proc. R. Soc. Lond. A* **465** (2009), 843–865.
- [Stephen and Ghosh 2005] N. G. Stephen and S. Ghosh, “Eigenanalysis and continuum modelling of a curved repetitive beam-like structure”, *Int. J. Mech. Sci.* **47** (2005), 1854–1873.
- [Stephen and Wang 2000] N. G. Stephen and P. J. Wang, “On transfer matrix eigenanalysis of pin-jointed frameworks”, *Comput. Struct.* **78** (2000), 603–615.
- [Stephen and Zhang 2004] N. G. Stephen and Y. Zhang, “Eigenanalysis and continuum modelling of an asymmetric beamlike repetitive structure”, *Int. J. Mech. Sci.* **46** (2004), 1213–1231.
- [Stephen and Zhang 2006] N. G. Stephen and Y. Zhang, “Eigenanalysis and continuum modeling of pre-twisted repetitive beam-like structures”, *Int. J. Solids Struct.* **43** (2006), 3832–3855.
- [Tej and Tejová 2014] P. Tej and A. Tejová, “Design of an experimental prestressed Vierendeel pedestrian bridge made of UHPC”, *Appl. Mech. Mater.* **587** (2014), 1642–1645.
- [Trovalusci et al. 2015] P. Trovalusci, M. Ostoja-Starzewski, M. L. De Bellis, and A. Murralli, “Scale-dependent homogenization of random composites as micropolar continua”, *Eur. J. Mech. A Solid.* **49** (2015), 396–407.
- [Wang and Stronge 1999] X. L. Wang and W. J. Stronge, “Micropolar theory for two-dimensional stresses in elastic honeycomb”, *Proc. R. Soc. Lond. A* **455**:1986 (1999), 2091–2116.
- [Warren and Byskov 2002] W. E. Warren and E. Byskov, “Three-fold symmetry restrictions on two-dimensional micropolar materials”, *Eur. J. Mech. A Solids* **21**:5 (2002), 779–792.

[Yong and Lin 1989] Y. Yong and Y. K. Lin, “Dynamics of complex truss-type space structures”, *AIAA J.* **28** (1989), 1250–1258.

[Zhong and Williams 1995] W. X. Zhong and F. W. Williams, “On the direct solution of wave propagation for repetitive structures”, *J. Sound Vib.* **181** (1995), 485–501.

Received 11 Oct 2016. Revised 21 Dec 2016. Accepted 26 Dec 2016.

ANTONIO GESUALDO: gesualdo@unina.it

Department of Structures for Engineering and Architecture, University of Naples Federico II, Via Claudio 21, 80125 Naples, Italy

ANTONINO IANNUZZO: antoninoiannuzzo@libero.it

Department of Structures for Engineering and Architecture, University of Naples Federico II, Via Claudio 21, 80125 Naples, Italy

FRANCESCO PENTA: penta@unina.it

Department of Industrial Engineering, University of Naples Federico II, Piazzale Tecchio 80, 80125 Naples, Italy

GIOVANNI PIO PUCILLO: gpucillo@unina.it

Department of Industrial Engineering, University of Naples Federico II, Piazzale Tecchio 80, 80125 Naples, Italy

JOURNAL OF MECHANICS OF MATERIALS AND STRUCTURES

msp.org/jomms

Founded by Charles R. Steele and Marie-Louise Steele

EDITORIAL BOARD

ADAIR R. AGUIAR	University of São Paulo at São Carlos, Brazil
KATIA BERTOLDI	Harvard University, USA
DAVIDE BIGONI	University of Trento, Italy
YIBIN FU	Keele University, UK
IWONA JASIUK	University of Illinois at Urbana-Champaign, USA
MITSUTOSHI KURODA	Yamagata University, Japan
C. W. LIM	City University of Hong Kong
THOMAS J. PENCE	Michigan State University, USA
GIANNI ROYER-CARFAGNI	Università degli studi di Parma, Italy
DAVID STEIGMANN	University of California at Berkeley, USA
PAUL STEINMANN	Friedrich-Alexander-Universität Erlangen-Nürnberg, Germany

ADVISORY BOARD

J. P. CARTER	University of Sydney, Australia
D. H. HODGES	Georgia Institute of Technology, USA
J. HUTCHINSON	Harvard University, USA
D. PAMPLONA	Universidade Católica do Rio de Janeiro, Brazil
M. B. RUBIN	Technion, Haifa, Israel

PRODUCTION production@msp.org

SILVIO LEVY Scientific Editor


Cover photo: Mando Gomez, www.mandolux.com

See msp.org/jomms for submission guidelines.

JoMMS (ISSN 1559-3959) at Mathematical Sciences Publishers, 798 Evans Hall #6840, c/o University of California, Berkeley, CA 94720-3840, is published in 10 issues a year. The subscription price for 2017 is US \$615/year for the electronic version, and \$775/year (+\$60, if shipping outside the US) for print and electronic. Subscriptions, requests for back issues, and changes of address should be sent to MSP.

JoMMS peer-review and production is managed by EditFLOW[®] from Mathematical Sciences Publishers.

PUBLISHED BY

 **mathematical sciences publishers**
nonprofit scientific publishing

<http://msp.org/>

© 2017 Mathematical Sciences Publishers

B-splines collocation for plate bending eigenanalysis	CHRISTOPHER G. PROVATIDIS	353
Shear capacity of T-shaped diaphragm-through joints of CFST columns	BIN RONG, RUI LIU, RUOYU ZHANG, SHUAI LIU and APOSTOLOS FAFITIS	373
Polarization approximations for elastic moduli of isotropic multicomponent materials	DUC CHINH PHAM, NGUYEN QUYET TRAN and ANH BINH TRAN	391
A nonlinear micromechanical model for progressive damage of vertebral trabecular bones	EYASS MASSARWA, JACOB ABOUDI, FABIO GALBUSERA, HANS-JOACHIM WILKE and RAMI HAJ-ALI	407
Nonlocal problems with local Dirichlet and Neumann boundary conditions	BURAK AKSOYLU and FATIH CELIKER	425
Optimization of Chaboche kinematic hardening parameters by using an algebraic method based on integral equations	LIU SHIJIE and LIANG GUOZHU	439
Interfacial waves in an A/B/A piezoelectric structure with electro-mechanical imperfect interfaces	M. A. REYES, J. A. OTERO and R. PÉREZ-ÁLVAREZ	457
Fully periodic RVEs for technological relevant composites: not worth the effort!	KONRAD SCHNEIDER, BENJAMIN KLUSEMANN and SWANTJE BARGMANN	471
Homogenization of a Vierendeel girder with elastic joints into an equivalent polar beam	ANTONIO GESUALDO, ANTONINO IANNUZZO, FRANCESCO PENTA and GIOVANNI PIO PUCILLO	485
Highly accurate noncompatible generalized mixed finite element method for 3D elasticity problems	GUANGHUI QING, JUNHUI MAO and YANHONG LIU	505
Thickness effects in the free vibration of laminated magneto-electroelastic plates	CHAO JIANG and PAUL R. HEYLIGER	521
Localized bulging of rotating elastic cylinders and tubes	JUAN WANG, ALI ALTHOBAITI and YIBIN FU	545